Available online at www.sciencedirect.com
ScienceDirect
ELSEVIER
Biochemical and Biophysical Research Communications 353 (2007) 764–769
BBRC
www.elsevier.com/locate/ybbrc

Signaling pathway of nitric oxide production induced by ginsenoside Rb1 in human aortic endothelial cells: A possible involvement of androgen receptor

Jing Yu [a], Masato Eto [b], Masahiro Akishita [b], Akiyo Kaneko [a], Yasuyoshi Ouchi [b], Tetsuro Okabe [a,*]

[a] *Department of Integrated Traditional Medicine, University of Tokyo Graduate School of Medicine, Tokyo, Japan*
[b] *Department of Gerontology, University of Tokyo Graduate School of Medicine, Tokyo, Japan*

Received 7 December 2006
Available online 22 December 2006

Abstract

Ginsenosides have been shown to stimulate nitric oxide (NO) production in aortic endothelial cells. However, the signaling pathways involved have not been well studied in human aortic endothelial cells. The present study was designed to examine whether purified ginsenoside Rb1, a major active component of ginseng could actually induce NO production and to clarify the signaling pathway in human aortic endothelial cells. NO production was rapidly increased by Rb1. The rapid increase in NO production was abrogated by treatment with nitric oxide synthetase inhibitor, L-NAME. Rb1 stimulated rapid phosphorylation of Akt (Ser473), ERK1/2 (Thr202/Thr204) and eNOS (Ser1177). Rapid phosphorylation of eNOS (Ser1177) was prevented by SH-5, an Akt inhibitor or wortmannin, PI3-kinase inhibitor and partially attenuated by PD98059, an upstream inhibitor for ERK1/2. Interestingly, NO production and eNOS phosphorylation at Ser1177 by Rb1 were abolished by androgen receptor antagonist, nilutamide. The results suggest that PI3kinase/Akt and MEK/ERK pathways and androgen receptor are involved in the regulation of acute eNOS activation by Rb1 in human aortic endothelial cells.

Keywords: Ginsenoside Rb1; Endothelial cells; Nitric oxide; eNOS; Androgen receptor; PI3-kinase; Akt; ERK; MEK; Phosphorylation

Ginseng, the root of Panax ginseng C.A. Meyer (Araliaceae), is a well-known and popular herbal medicine used worldwide. Among more than 30 ginsenosides, the active ingredient of ginseng, ginsenoside Rb1 is regarded as the main compound responsible for many pharmaceutical actions of ginseng. The oral administration of ginseng caused a decrease in blood pressure in essential hypertension [1]. Intravenous administration of ginsenosides (a mixture of saponin from Panax ginseng C.A. Meyer) lowered blood pressure in a dose-dependent manner in anesthetized rats [2]. Although these reports suggest that ginsenosides could stimulate the production of nitric oxide (NO) by aortic vascular endothelial cells, the precise mechanisms of the ginsenoside actions have not been fully elucidated [3]. NO released from endothelial cells via the endothelial nitric oxide synthetase (eNOS) is a pivotal vasoprotective molecule. In addition to its vasodilating feature, endothelial NO has anti-atherosclerotic properties, such as inhibition of platelet aggregation, leukocyte adhesion, smooth muscle cell proliferation, and expression of genes involved in atherosclerosis [4].

The present study aims at investigating the signaling pathways involved in NO production by purified ginsenoside Rb1 in human aortic endothelial cells in vitro.

Materials and methods

Materials. Rb1, nilutamide, L-NAME (hydrochloride), Hanks' balanced salt solution (HBSS) were purchased from Sigma (St. Louis, MO,

* Corresponding author. Fax: +813 5684 3987.
E-mail address: okabe-tky@umin.ac.jp (T. Okabe).

0006-291X/$ - see front matter © 2006 Elsevier Inc. All rights reserved.
doi:10.1016/j.bbrc.2006.12.119

USA). ICI182780 was from Zeneca Pharmaceuticals (Macdesfield, UK). 4,5-diaminofluorescin diacetate (DAF-2 DA) was purchased from Daiichi (Daiichi Pure Chemicals Co., Ltd, Tokyo, Japan). PD98059, SH-5, wortmannin and Nitric Oxide Synthase Assay Kit were from Calbiochem (EDM Biosciences, Inc., La Jolla, CA, USA and Germany). L-[^{3}H]Arginine was purchased from Amersham (Amersham Biosciences, Uppsala, Sweden). Antibody of phospho-eNOS (Ser1177) was from upstate (Upstate Inc., Lake Placid, NY). Antibody for eNOS/NOS type III was purchased form BD Transduction Laboratories (BD Biosciences, Franklin Lakes, NJ, USA). All other antibodies were form Cell Signaling Technology (Beverly, MA, USA). LumiGLO Reserve Chemiluminescent Substrate Kit was from KPL (Gaithersburg, MD, USA). EBM-2 (endothelial cell base medium) was from Clonetics (Walkersville, MD, USA). Human aortic endothelial cells (HAECs) were from Cambrex (Cambrex BioScience Walkersville, Inc. Walkersville, MD, USA). Fetal bovine serum (FBS) was from CCT (Sanko Junyaku Co., Ltd, Tokyo, Japan), Fetal bovine serum charcoal stripped was from MultiSer (ThermoTrace Ltd., Melbourne, Australia).

Cell culture. HAECs were cultured in a 37 °C humidified atmosphere of 95% air/5% CO_2 in EGM-2 (endothelial cell grows medium 2) medium supplemented with 10% FBS. The EGM-2 medium consisted of 0.1% EGF, 0.04% hydrocortisone, 0.4% hFGF-B, 0.1% VEGF, 0.1% R^3-IGF-1, 0.1% ascorbic acid, 0.1% GA-1000, and 0.1% heparin. Experiments were performed with cells from passages 5 to 7. For all experiments, HAECs were plated at a concentration of 1×10^4/mL and grown to confluence. Then cells were serum-starved for 6 h in phenol red free EBM-2 containing 1% DCC-FBS, that was removed the steroid by processing it with dextran-coated charcoal (DCC-FBS). In some inhibitory experiments, the inhibitors were added to cells 60 min before the stimuli. DMSO was used as a solvent for Rb1, PD98059, wortmannin, SH-5, L-NAME, nilutamide, and DAF-2 DA present at equal concentrations (0.01%) in all groups, including the vehicle.

Western blot analysis. After treatment with reagents, confluent monolayers of cells were washed two times in ice-cold phosphate-buffered saline and lysed with buffer containing 20 mmol/L Tris–HCl (pH 7.5), 150 mmol/L NaCl, 1 mmol/L EDTA, 1 mmol/L EGTA, 1% Triton-X, 2.5 mmol/L sodium pyrophosphate, 1 mmol/L β-glycerophosphate, 1 mmol/LNa_3VO_4, 1 μg/mL Leupeptin, 1 mM PMSF). For western blot analysis, total cell lysate was subjected to SDS–polyacrylamide gel electrophoresis (PAGE), and proteins were transferred to poly vinilidene difluoride (PVDF) membrane. The antibodies used in this study were anti-phospho-ERK1/2 (Thr202/Thr204), anti-ERK1/2, anti phospho-Akt (Ser473), anti-Akt, anti-phosph-eNOS (ser1177) and anti-NOS. Antibodies were detected by means of a horseradish peroxidase-linked secondary antibody and immunoreactive bands were visualized using LumiGLO Reserve Chemiluminescent Substrate Kit.

Endothelial NO synthase activity assay. Endothelial cell NO synthase (eNOS) activity was quantified by measuring the conversion of L-[^{3}H]-arginine to L-[^{3}H]-citrulline by the use of a NO synthase assay kit.

Measurement of intracellular production of NO. Production of NO was assessed using the NO-sensitive fluorescent dye DAF-2 DA [5]. Briefly, confluent cells were serum-staved for 6 h. Because NOS generates O_2^- instead of NO in the absence of L-arginine, so L-arginine (100 μmol/L) was add 1 h prior to all solutions, except for the experiment with *N*-nitro-L-arginine methyl ester (L-NAME; a NOS inhibitor)-treated cells. Cells were loaded with DAF-2 DA (final concentration 5 μmol/L, 30 min 37 °C) and than rinsed three times with HBSS, kept in the dark, and maintained at 37 °C in 1% EBM-2 medium with a warming stage. After 30 min, cells were then treated with Rb1 or other stimuli. In some inhibitory experiments, the inhibitors were administered 30 min before loading with DAF-2 DA. Green fluorescence intensity was measured with a laser scanning confocal microscopy system (LSCM) (Bio-Rad Laser Sharp2000). The fluorescence image was obtained as a 512 × 512 pixel frame. Ex = 488 nm, EM = 510 nm. All other settings, including scanning speed, pinhole diameter, and voltage gain, remained the same for all experiments.

Statistics. Data are means ± SEM. Statistical comparisons were performed by Student's *T* test between two groups. A value of $P < 0.05$ was considered significant.

Results

Rb1 stimulates rapid production of NO in human aortic endothelia cells

We used the NO-specific fluorescent dye DAF-2 DA to evaluate the effect of Rb1 on NO production in HAECs. 5, 10, 15, 30, 60, 120 and 180 min after Rb1 treatment, cells were fixed and then viewed using a fluorescence microscope. Emission of green light (510 nm) from cells excited by light at 488 nm is indicative of NO production. A significant increase in green fluorescence was observed >15 min after the addition of Rb1 and lasted for 60 min in HAECs (Fig. 1A). Maximal stimulation of NO production was obtained at 30 min.

To verify that the rapid increase in green fluorescence in response to Rb1 treatment specifically reflected NO production, we compared results from HAECs treated with acetylcholine (1 μmol/L) or Rb1 (1 μmol/L) for 5 min. Reassuringly, treatment with either acetylcholine and calcium ionophore or Rb1 resulted in a increase in green fluorescence (Fig. 1B). We next examined the effects of the NOS inhibitor L-NAME to determine whether the NO increase was attributable to NOS derived de novo synthesis. As shown in Fig. 1C, the Rb1-induced DAF-2 DA fluorescence was completely suppressed by pretreatment with L-NAME (0.5 mmol/L). The results suggested that the rapid increase in NO production after Rb1 treatment was mediated by an increase in NOS activity.

Rb1 stimulates phosphorylation of eNOS (Ser1177) and increases NOS activity

To examine involvement of eNOS in the NO increase, the effect of Rb1 on eNOS phosphorylation at Ser-1177 was tested by Western blotting. As shown in Fig. 2, Rb1 induced rapid eNOS phosphorylation after 10 min of incubation, maximal eNOS phosphorylation by Rb1 was observed from 30 to 60 min of incubation. The relative magnitude of eNOS phosphorylation falls subsequently but is still significantly greater than control after 120 min of Rb1 incubation (Fig. 2A, upper blots). The acute effect by Rb1 on eNOS phosphorylation was concentration dependent (Fig. 2B, upper blots). Rb1 did not affect eNOS protein expression (Fig. 2A and B, lower blots).

To see whether Rb1 actually activates NOS in HAECs, we measured NOS activity after 30 min of treatment with Rb1. As shown in Fig. 2C, Rb1 significantly increased NOS activity in HAECs.

PI3-kinase/Akt and MEK/ERK pathways are involved in eNOS phosphorylation and NO production

Previous studies have demonstrated that PI3-kinase/Akt and MEK/ERK pathways are two important signaling cascades mediating eNOS activation by many stimuli in vascular endothelial cells [6,7]. Therefore, we examined

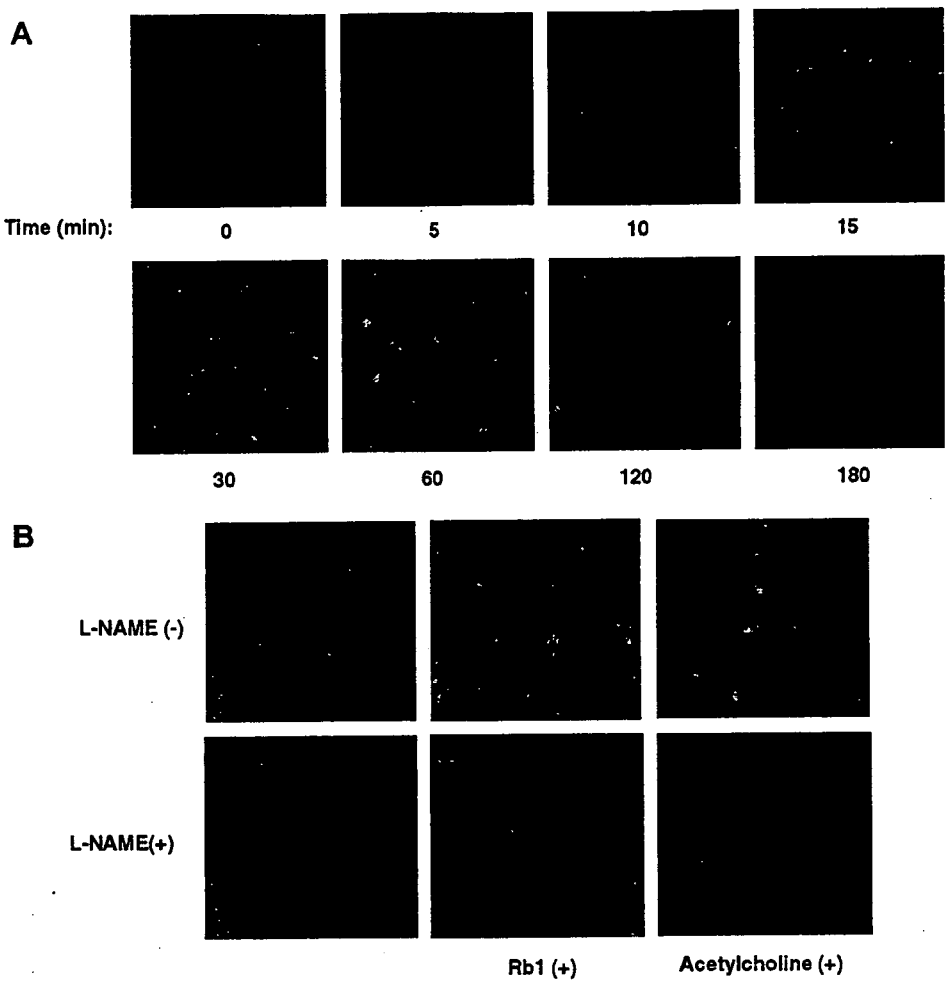

Fig. 1. Effect of Rb1 on production of NO. HAECs were starved and loaded with DAF-2 DA (5 μmol/L) as described in Materials and methods prior to treatment with either Rb1 (1 μmol/L) for 0, 5, 10, 15, 30, 60, 120, and 180 min (A) or acetylcholine (1 μmol/L) for 5 min (B). After Rb1 treatment, cells were fixed in 2% paraformaldehyde for 10 min at 4 °C and then viewed using a fluorescent microscope. Emission of green light (510 nm) from cells excited by light at 488 nm is indicative of NO production. In some groups of cells, L-NAME (0.5 mmol/L) was added 30 min before loading cells with DAF-2 DA (B). A representative time course experiment is shown for experiments that were repeated independently for three times. (For interpretation of the references to color in this figure legend, the reader is referred to the web version of this paper.)

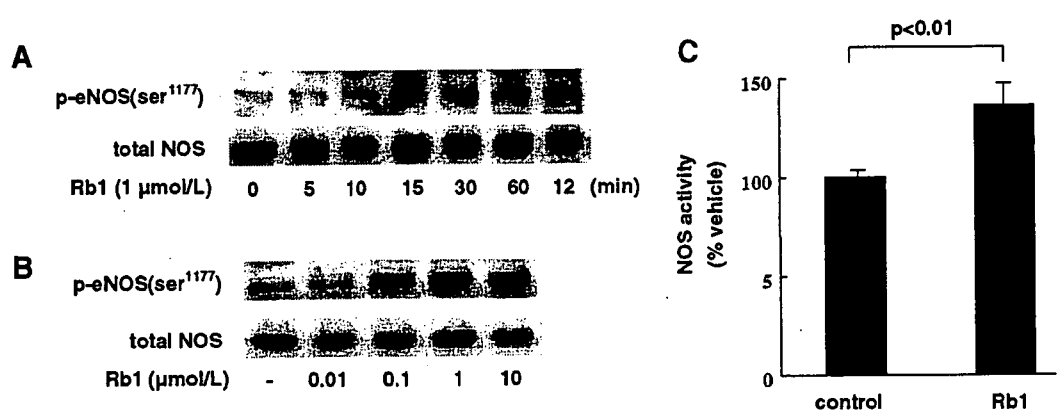

Fig. 2. Effects of Rb1 on eNOS phosphorylation and NOS activity. Phosphorylation of eNOS in HAECs. Starved HAECs were treated with the vehicle (0.01% DMSO) or Rb1 (1 μmol/L) for indicated times (A) or with various concentrations of Rb1 for 30 min (B). Western analysis performed to detect phospho-eNOS (Ser1177) and total eNOS. The experiments were repeated three times in triplicates, with equal result. NOS activity in HAECs homogenates. Rb1 (1 μmol/L) were added to the starved medium for 30 min, then activity of NOS was measured by the conversion of L-arginine to L-citrulline at 37 °C for 60 min (C). Histograms and error bars represent means ± SEM of four independent experiments performed in duplicate. $^{*}P < 0.01$ vs control.

whether Rb1 activated Akt and ERK1/2. We used phospho-specific antibodies to evaluate the ability of Rb1 to stimulate phosphorylation of Akt and ERK1/2 in HAECs. Rb1 rapidly increased phosphorylation of Akt (Ser473) and ERK1/2 (Fig. 3A, upper blots) in HAECs > 5 min after the addition of Rb1. Maximal phosphorylation was attained at 30 min in Akt and at 15 min in ERK1/2. The relative magnitude of the Rb1 response falls subsequently but is still significantly greater than control after 120 min of Rb1 treatment. Rb1 did not affect total Akt and ERK protein expression (Fig. 3A, lower blots).

We next examined the rapid phosphorylation of eNOS at Ser1179 by Rb1 either in the absence or presence of PI3 kinase inhibitor wortmannin, and Akt inhibitor SH-5 or MEK (ERK kinase) inhibitor PD98059. As shown in Fig. 3B, the rapid eNOS phosphorylation was abolished by pretreatment of cells with wortmannin (5 μmol/L) or SH-5, and partially attenuated by MEK inhibitor PD98059 (10 μmol/L). NO production viewed by fluorescent microscopy showed the similar inhibition by these inhibitors (Fig. 3C). These results suggest that acute activation of eNOS and NO production by Rb1 were mediated through activation of PI3-kinase/Akt and ERK1/2.

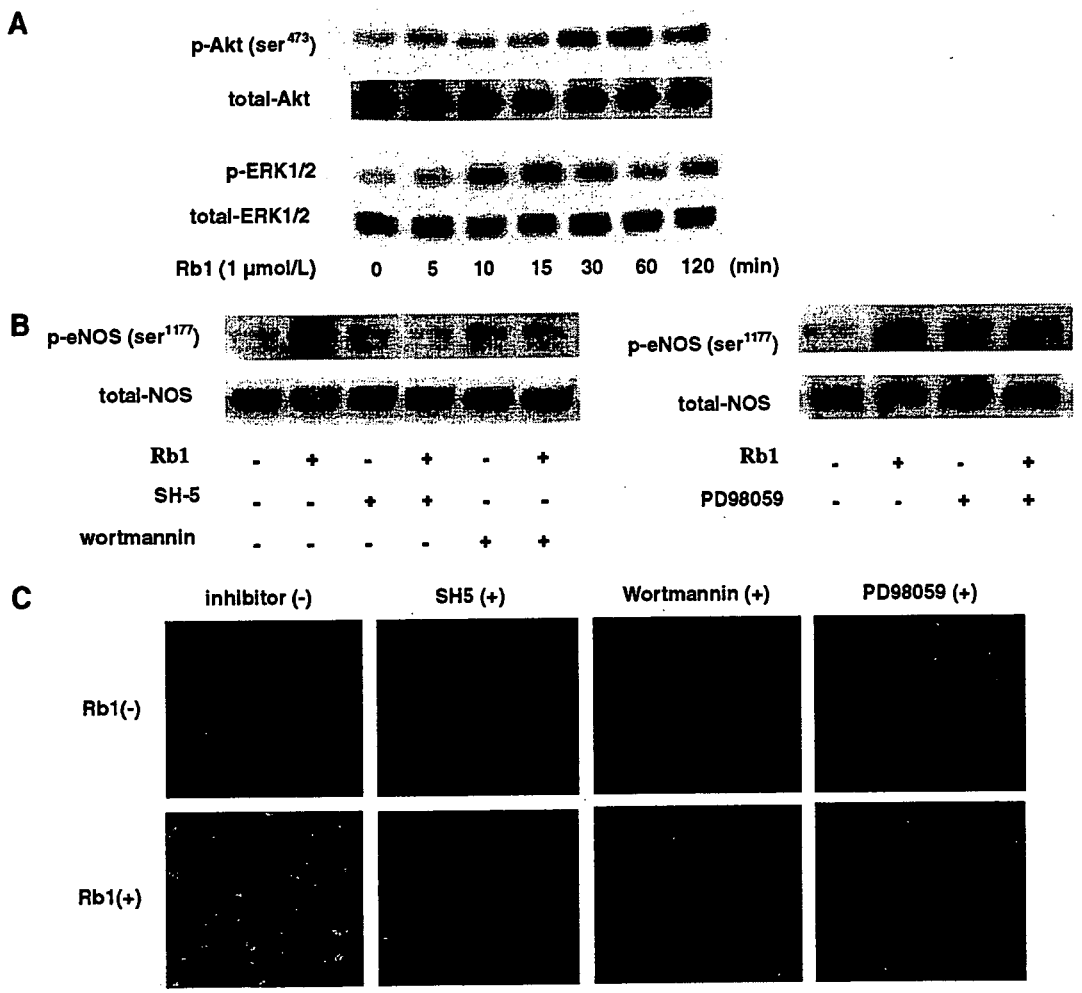

Fig. 3. Effects of inhibitors for PI3kinae/Akt or MEK (ERK kinase) on eNOS phosphorylation and NO production. Starved HAECs were treated with the vehicle (0.01% DMSO) or Rb1 (1 μmol/L) for indicated times (A). In some groups, cells were pretreated with SH-5 (10 μmol/L), wortmannin (5 μmol/L) or PD98059 (10 μmol/L) for 1 h, then cells were treated without or with Rb1 (1 μmol/L) for 30 min (B). Cell lysates were analyzed by Western blot as described in Materials and methods. Anti-phospho-Akt (Ser473) antibody and anti-Akt antibody; anti-phospho-ERK1/2 antibody and anti-ERK1/2 antibody (A), anti-phospho-eNOS (Ser1177) antibody and anti-eNOS antibody (B) were used for western blot analysis. Experiments were repeated three times, with equivalent result. Starved cells were loaded with DAF-2 DA as described in Materials and methods before treatment with Rb1 (1 μmol/L). In some groups of cells, SH-5 (10 μmol/L), wortmannin (5 μmol/L) or PD98059 (10 μmol/L) were added 60 min before cells were loaded with DAF-2 DA. After Rb1 treatment, cells were fixed in 2% paraformaldehyde for 10 min at 4 °C and then viewed using a fluorescent microscope (C). Emission of green light (510 nm) from cells excited by light at 488 nm is indicative of NO production. A representative set of experiments is shown for experiments that were repeated independently three times. (For interpretation of the references to color in this figure legend, the reader is referred to the web version of this paper.)

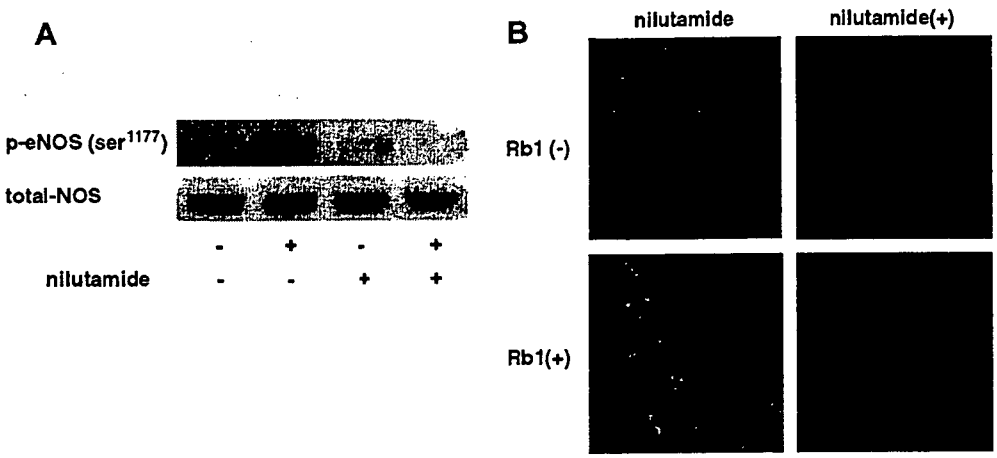

Fig. 4. Effects of nilutamide, an antagonist of androgen receptor, on eNOS phosphorylation and NO production. HAECs were starved 6 h and then treated without or with Rb1 (1 μmol/L) for 30 min. Some groups of cells were pre-treated with androgen receptor agonist nilutamide (10 μmol/L) for 1 h. Cell lysates were then subjected to immunoblotting as described in Materials and methods. The experiments were repeated three times in triplicates, with equal results. Starved cells were loaded with DAF-2 DA as described in Materials and methods before treatment with Rb1 (1 μmol/L). In some groups of cells, nilutamide (10 μmol/L) were added 60 min before cells were loaded with DAF-2 DA. After Rb1 treatment, cells were fixed in 2% paraformaldehyde for 10 min at 4 °C and then viewed using a fluorescent microscope (B). Emission of green light (510 nm) from cells excited by light at 488 nm is indicative of NO production. The experiments were repeated independently three times with equal results. (For interpretation of the references to color in this figure legend, the reader is referred to the web version of this paper.)

Rb1-induced eNOS phosphorylation is inhibited by androgen receptor antagonist

Increasing evidence shows that activation of the steroid hormone receptor such as estrogen receptor (ER) lead to NO production and vasodilation within minutes by non-transcriptional pathways. Ginsenosides have steroidal skeleton structure and can act as an agonist for steroid hormones receptor. To see whether steroid hormone receptors were involved in acute activation of eNOS to produce NO in HUACs by Rb1, we examined the effects of the androgen receptor antagonist nilutamide and estrogen receptor antagonist ICI182780. Representative western blots obtained using anti-phospho-eNOS (Ser1177) antibody and anti-eNOS antibody are shown in Fig. 4A. The Rb1-induced eNOS phosphorylation (Ser1177) was inhibited by the androgen receptor antagonist nilutamid (10 μmol/L) In addition, NO production was diminished to the baseline level in the presence of nilutamid (Fig. 4B). However, the Rb1-induced eNOS phosphorylation (Ser1177) and NO production were unaffected by an estrogen receptor (ER) antagonist ICI182780 (10 μmol/L) (data not shown).

Discussion

We have shown that purified Rb1 rapidly stimulates production of NO in HAECs > 15 min after treatment. Maximal stimulation of NO production was obtained at 30 min. The increase in NO production was abrogated by the addition of eNOS inhibitor, L-NAME. It is generally well known that eNOS is tightly regulated not only at the transcriptional level but also by several post-transcriptional mechanisms [8]. The enhanced phosphorylation at Ser1177 leads to increased eNOS activity. In our experiments, Rb1 induced rapid phosphorylation of eNOS at Ser1177 > 10 min after Rb1 treatment. Maximal eNOS phosphorylation by Rb1 was observed from 30 to 60 min of incubation. NOS activity was also increased by the addition of Rb1 in HAECs. Taken together, our results suggest that the acute effect on NO production in HAECs is attributable to rapid phosphorylation of eNOS at Ser1177. NO produced by eNOS is a fundamental determinant of cardiovascular homeostasis responsible for regulating systolic blood pressure, vascular remodeling and angiogenesis. It is possible to consider that Rb1, a major active component of ginseng could be a candidate responsible for the antihypertensive effects of ginseng previously reported [1,2].

Recent studies have revealed that PI3-kinase/Akt and MEK/ERK1/2 pathways are crucial regulator in cell proliferation, cell-cycle progression, and mediator of cellular survival. Both of them also contribute to enhanced phosphorylation of eNOS at Ser1177/1179 and production of NO [6,7]. The present study showed that Rb1 also stimulated the phosphorylation of Akt (Ser473) and ERK1/2 (Thr202/Thr204) in HAECs. Rb1-induced eNOS phosphorylation was prevented by inhibitors for PI3-kinase/Akt or MEK (ERK kinase). Our data suggest that the activation of PI3-kinase/Akt and MEK/ERK-mediated pathways are involved in the regulation of acute eNOS phosphorylation by ginsenoside Rb1 in HAECs.

Another interesting finding is that acute phosphorylation of eNOS by Rb1 was abolished by an antagonist for androgen receptor. Recent studies have shown Rb1 acts as a phytoestrogen in MCF-7 human mammary carcinoma

cells [9]. However, in HAECs, Rb1-induced eNOS phosphorylation was not prevented by an antagonist for estrogen receptor (data not shown). It is known that testosterone prevents coronary artery disease, and lower testosterone level is a risk factor for ischemic heart disease in men [10–12]. Recent studies revealed that endothelial NO has antiatherosclerotic properties, such as inhibition of platelet aggregation, leukocyte adhesion, smooth muscle cell proliferation, and expression of genes involved in atherosclerosis [4]. Together with these observations, our results that Rb1 induced eNOS phosphorylation has been abolished by the androgen receptor antagonist will be the beginning of the experimental analyses at cellular levels and may provide a clue for better understanding of the mechanisms by which androgens exert their action for preventing coronary artery disease. Further studies are required for elucidation.

Acknowledgments

We thank Drs. K. Yamamoto, K. Hasegawa, Y. Iwaoka, and S. Takasugi for their helpful advices and continuous encouragement.

References

[1] K.H. Han, S.C. Choe, H.S. Kim, D.W. Sohn, K.Y. Nam, B.H. Oh, M.M. Lee, Y.B. Park, Y.S. Choi, J.D. Seo, Y.W. Lee, Effect of red ginseng on blood pressure in patients with essential hypertension and white coat hypertension, Am. J. Chin. Med. 26 (1998) 199–209.

[2] N.D. Kim, S.Y. Kang, V.B. Schini, Ginsenosides evoke endothelium-dependant vascular relaxation in rat aorta, Gen. Pharmacol. 25 (1994) 1071–1077.

[3] N.D. Kim, S.Y. Kang, J.H. Park, V.B. Schini-Kerth, Ginsenoside Rg3 mediates endothelium-dependent relaxation in response to ginsenosides in rat aorta: role of K^+ channels, Eur. J. Pharmacol. 367 (1999) 41–49.

[4] A.G. Herman, S. Moncada, Therapeutic potential of nitric oxide donors in the prevention and treatment of atherosclerosis, Eur. Heart J. 26 (2005) 1945–1955.

[5] H. Kojima, N. Nakatsubo, K. Kikuchi, S. Kawahara, Y. Kirino, H. Nagoshi, Y. Hirata, T. Nagano, Detection and imaging of nitric oxide with novel fluorescent indicators: diaminofluoresceins, Anal. Chem. 70 (1998) 2446–2453.

[6] X. Peng, S. Haldar, S. Deshpande, K. Irani, D.A. Kass, Wall stiffness suppresses Akt/eNOS and cytoprotection in pulse-perfused endothelium, Hypertension 41 (2003) 378–381.

[7] D. Feliers, X. Chen, N. Akis, G.G. Choudhury, M. Madaio, B.S. Kasinath, VEGF regulation of endothelial nitric oxide synthase in glomerular endothelial cells, Kidney Int. 68 (2005) 1648–1659.

[8] I. Fleming, R. Busse, Molecular mechanisms involved in the regulation of the endothelial nitric oxide synthase, Am. J. Physiol. Regul. Integr. Comp. Physiol. 284 (2003) R1–R12.

[9] J. Cho, W. Park, S. Lee, W. Ahn, Y. Lee, Ginsenoside-Rb1 from Panax ginseng C.A. Meyer activates estrogen receptor-alpha and -beta, independent of ligand binding, J. Clin. Endocrinol. Metab. 89 (2004) 3510–3515.

[10] G.B. Phillips, B.H. Pinkernell, T.Y. Jing, The association of hypotesteronemia with coronary artery disease in men, Arterioscler. Thromb. 14 (1994) 701–706.

[11] C.M. Webb, J.G. McNeill, C.S. Hayward, D. De Zeigler, P. Collins, Effects of testosterone on coronary vasomotor regulation in men with coronary heart disease, Circulation 100 (1999) 1690–1696.

[12] F.C. Wu, A. von Eckardstein, Androgens and coronary artery disease, Endocr. Rev. 24 (2003) 183–217.

Available online at www.sciencedirect.com
ScienceDirect
European Journal of Pharmacology 556 (2007) 1–8
www.elsevier.com/locate/ejphar

Gas6/Axl-PI3K/Akt pathway plays a central role in the effect of statins on inorganic phosphate-induced calcification of vascular smooth muscle cells

Bo-Kyung Son [a], Koichi Kozaki [b], Katsuya Iijima [a], Masato Eto [a], Toru Nakano [c], Masahiro Akishita [a], Yasuyoshi Ouchi [a,*]

[a] *Department of Geriatric Medicine, Graduate School of Medicine, The University of Tokyo, 7-3-1 Hongo, Bunkyo-ku, Tokyo 113-8655, Japan*
[b] *Department of Geriatric Medicine, Kyorin University School of Medicine, Tokyo, Japan*
[c] *Discovery Research Laboratory, Shionogi and Co., Ltd., Osaka, Japan*

Received 19 May 2006; received in revised form 22 September 2006; accepted 27 September 2006
Available online 18 October 2006

Abstract

Apoptosis is essential for the initiation and progression of vascular calcification. Recently, we showed that *3-hydroxy-3-methylglutaryl* (HMG) CoA reductase inhibitors (statins) have a protective effect against vascular smooth muscle cell calcification by inhibiting apoptosis, where growth arrest-specific gene 6 (Gas6) plays a pivotal role. In the present study, we clarified the downstream targets of Gas6-mediated survival signaling in inorganic phosphate (Pi)-induced apoptosis and examined the effect of statins. We found that fluvastatin and pravastatin significantly inhibited Pi-induced apoptosis and calcification in a concentration-dependent manner in human aortic smooth muscle cells (HASMC), as was found with atorvastatin previously. Gas6 and its receptor, Axl, expression were downregulated in the presence of Pi, and recombinant human Gas6 (rhGas6) significantly inhibited apoptosis and calcification in a concentration-dependent manner. During apoptosis, Pi suppressed Akt phosphorylation, which was reversed by rhGas6. Wortmannin, a specific *phosphatidylinositol 3-OH kinase* (PI3K) inhibitor, abolished the increase in Akt phosphorylation by rhGas6 and eliminated the inhibitory effect of rhGas6 on both Pi-induced apoptosis and calcification, suggesting that PI3K-Akt is a downstream signal of the Gas6-mediated survival pathway. Pi reduced phosphorylation of Bcl2 and Bad, and activated caspase 3, all of which were reversed by rhGas6. The inhibitory effect of statins on Pi-induced apoptosis was accompanied by restoration of the Gas6-mediated survival signal pathway: upregulation of Gas6 and Axl expression, increased phosphorylation of Akt and Bcl2, and inhibition of Bad and caspase 3 activation. These findings indicate that the Gas6-mediated survival pathway is the target of statins' effect to prevent vascular calcification.

Keywords: Calcification; Apoptosis; Gas6; Axl; Akt; Bcl2

1. Introduction

Vascular calcification, such as coronary and aortic calcification, is clinically important in the development of cardiovascular disease (Eggen, 1968). Two distinct forms of vascular calcification are well recognized. One is medial calcification, which occurs between the cell layers of smooth muscle cells and is related to aging, diabetes and chronic renal failure (Neubauer, 1971; Goodman et al., 2000). The other is atherosclerotic calcification, which occurs in the intima during the development of atheromatous disease (Wexler et al., 1996). In diabetic patients, medial calcification has been shown to be a strong independent predictor of cardiovascular mortality (Everhart et al., 1988).

We recently demonstrated that atorvastatin prevented inorganic phosphate (Pi)-induced calcification by inhibiting apoptosis, one of the important processes regulating calcification. This was mediated by growth arrest-specific gene 6 (Gas6), a vitamin K-dependent protein (Son et al., 2006). Gas6 binds to Axl, the predominant receptor for Gas6, on the cell surface and transduces the signal by Axl autophosphorylation (Mark et al., 1996). Gas6-Axl interaction has been shown to be implicated in the regulation of multiple cellular functions (Yanagita et al., 2001; Goruppi et al., 1996; Nakano et al., 1997; Fridell et al., 1998). Especially, they are known to protect a range of cell types

* Corresponding author. Tel.: +81 3 5800 8652; fax: +81 3 5800 6530.
E-mail address: youchi-tky@umin.ac.jp (Y. Ouchi).

0014-2999/$ - see front matter © 2006 Elsevier B.V. All rights reserved.
doi:10.1016/j.ejphar.2006.09.070

from apoptotic death (Goruppi et al., 1996, 1999; Healy et al., 2001). However, the downstream targets of Gas6-mediated signaling in Pi-induced apoptosis and the effect of statins on this pathway are poorly understood.

With respect to the targets of Gas6-Axl interaction, Lee et al. (2002) showed that activation of Akt is necessary for Gas6-dependent cell survival. Akt is an important mediator of metabolic and survival responses after growth factor stimulation. Akt is activated by phosphorylation, which is performed by phosphatidylinositol 3-OH kinase (PI3K), a kinase that is activated by Gas6-Axl interaction (Lee et al., 2002; Ming Cao et al., 2001). Activation of Akt leads to downstream signaling events including those associated with mitochondrial regulators of apoptosis such as Bcl2 and Bad.

In the present study, we examined the effect of statins using two different types: lipophilic fluvastatin and hydrophilic pravastatin. We investigated the effect of statins on Pi-induced apoptosis and calcification as well as on signaling components in this process. Consequently, we found that both statins restored the Gas6-mediated survival pathway, with upregulation of the expression of Gas6 and Axl, increased phosphorylation of Akt, Bcl2 and Bad; and finally inhibition of caspase 3 activation, resulting in the prevention of apoptosis and subsequent calcification in human aortic smooth muscle cells (HASMC).

2. Materials and methods

2.1. Materials

Pravastatin and fluvastatin were supplied by Sankyo Co. Ltd. and Tanabe Seiyaku Co., Ltd., respectively. Recombinant human Gas6 (rhGas6) was prepared as described previously (Ming et al., 2001). Wortmannin was purchased from Calbiochem. All other reagents were of analytical grade.

2.2. Cell culture

HASMC were obtained from Clonetics. They were cultured in Dulbecco's modified Eagle's medium (DMEM) supplemented with 20% *fetal bovine serum* (FBS), 100 U/ml penicillin and 100 mg/ml streptomycin at 37 °C in a humidified atmosphere with 5% CO_2. HASMC were used up to passage 8 for the experiments.

2.3. Induction and quantification of calcification

For Pi-induced calcification, Pi (a mixed solution of Na_2HPO_4 and NaH_2PO_4 whose pH was adjusted to 7.4) was added to serum-supplemented DMEM to a final concentration of 2.6 mM. After the indicated incubation period, cells were decalcified with 0.6 M HCl, and Ca content in the supernatant was determined by the *o*-cresolphthalein complexone method (C-Test, WAKO). The remaining cells were solubilized in 0.1 M NaOH/0.1% *sodium dodecyl sulfate* (SDS), and cell protein content was measured by Bio-Rad protein assay. Calcification was visualized by von Kossa's method. Briefly, the cells were fixed with 4% formaldehyde and exposed to 5% aqueous $AgNO_3$.

2.4. Induction and determination of apoptosis

Two different time courses were tested to investigate Pi-induced apoptosis and examine the effect of statins, under short-term (within 24 h) and long-term (up to 10 days) conditions (Son et al., 2006).

2.4.1. TdT-mediated dUTP nick end-labeling (TUNEL) assay

TUNEL assay to detect DNA fragmentation was performed using a commercially available kit (ApopTag Plus, Chemicon). Briefly, the samples were preincubated with equilibration buffer for 10 min, and subsequently incubated with terminal deoxyribonucleotidyl transferase in the presence of digoxigenin-conjugated dUTP for 1 h at 37 °C. The reaction was terminated by incubating the samples in stopping buffer for 30 min. After 3 rinses with *phosphate-buffered saline* (PBS), a fluorescein-labeled anti-digoxigenin antibody was applied for 30 min, and the samples were rinsed 4 times with PBS. The samples were then stained, mounted with DAPI (*4′,6-diamino-2-phenylindole*)/antifade, and examined by fluorescence microscopy.

2.4.2. Detection of DNA fragmentation by ELISA

Cytoplasmic histone-associated DNA fragments were determined with a cell-death detection ELISA^{plus} kit (Roche) as a quantitative index of apoptosis. Briefly, after the cells were incubated in lysis buffer for 30 min, 20 μl of the cell lysates was used for the assay. Following addition of substrate, colorimetric change was determined as the absorbance value measured at 405 nm.

2.5. Immunoblotting

The effect of Pi and statins on the expression of Gas6 and Axl, phosphorylation of Akt, Bcl2 and Bad, and activation of caspase 3 was examined at 12 h. The collected cell lysates were applied to SDS-polyacrylamide gels under reducing conditions, and transferred to a polyvinylidene difluoride (PVDF) membrane. Immunoblot analysis was performed using specific primary antibodies: anti-Axl, anti-Gas6 (Santa Cruz Biotechnology), anti-caspase 3, anti-Akt, anti-Bcl2, anti-phospho-Akt, anti-phospho-Bcl2, anti-phospho-Bad (Cell Signaling Technology), and anti-Bad (Transduction Laboratories). After incubation with horseradish peroxidase-conjugated secondary antibodies (Amersham Pharmacia), blots were visualized by enhanced chemiluminescence and autoradiography (ECL Plus, Amersham Pharmacia). Experiments were performed with at least three different cell populations.

2.6. Statistical analysis

All results are presented as mean± S.E.M. Statistical comparisons were made by ANOVA, unless otherwise stated. A value of $P<0.05$ was considered to be significant.

3. Results

3.1. Statins inhibit Pi-induced apoptosis and calcification in HASMC

In HASMC, a high Pi level (≥2.6 mM), comparable to that of hyperphosphatemia in end-stage renal disease, significantly induced calcification. Fluvastatin showed an inhibitory effect on Pi-induced calcification at as high a concentration as 0.1 μM (26.1±2.3% of control), while pravastatin showed the degree of effect at 50 μM (27.4±3.1% of control) (Fig. 1A). An inhibitory effect on Ca deposition was also found by von Kossa's staining (Fig. 1B). Both statins prevented Pi-induced apoptosis at the same concentrations as those at which they prevented calcification (Fig. 1C). An antiapoptotic effect of statins was also observed by TUNEL assay on day 6 (Fig. 1D).

3.2. Gas6 plays an important role in Pi-induced apoptosis

In the presence of 2.6 mM Pi, the expression of Gas6 and Axl was markedly downregulated (Fig. 2A). To investigate the role of Gas6 in Pi-induced apoptosis and calcification, first, we tested whether supplementation of rhGas6 could prevent Pi-induced apoptosis. In HASMC, rhGas6 significantly inhibited Pi-induced apoptosis in a concentration-dependent manner (Fig. 2B). Furthermore, during apoptosis, activated products of caspase 3 (17 and 19 kDa) were significantly increased by 2.6 mM Pi, which was reversed by rhGas6 (Fig. 2C). Next, we examined the effect of rhGas6 on calcification. Recombinant human Gas6 significantly inhibited Pi-induced calcification on day 6 in a concentration-dependent manner (Fig. 2D), suggesting that Gas6 plays an important role in Pi-induced apoptosis and calcification.

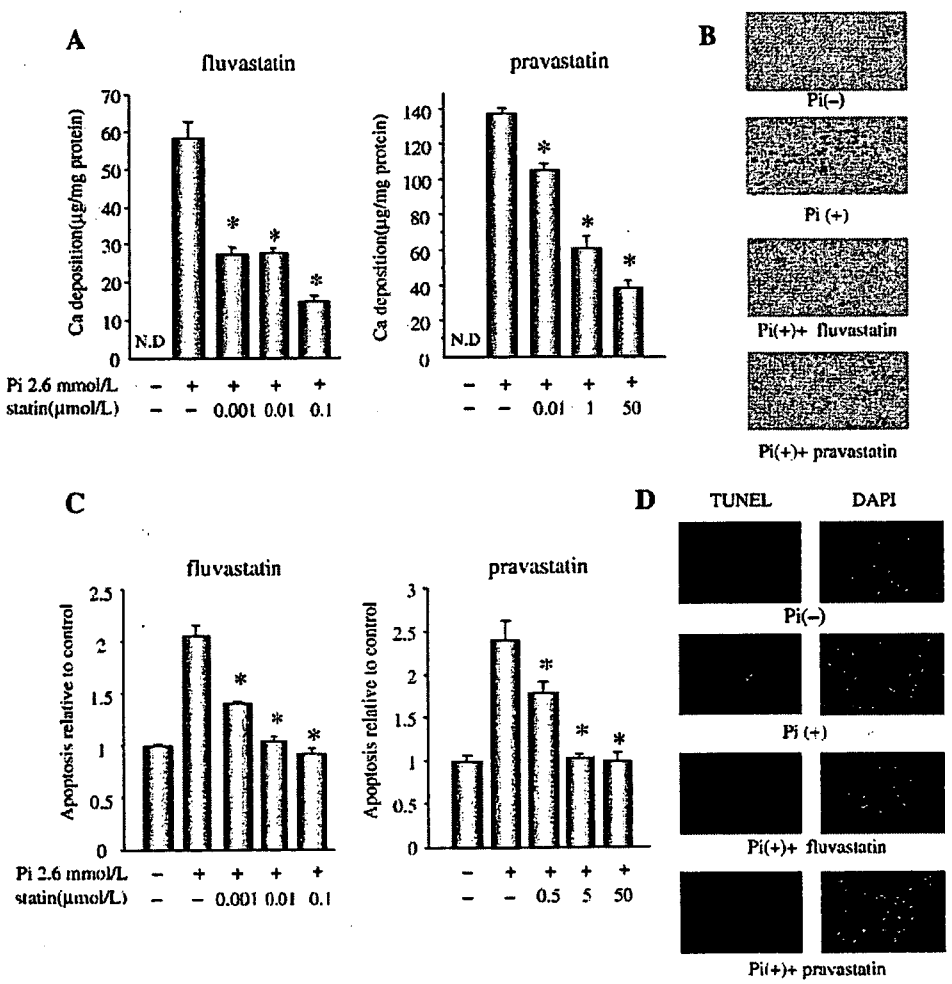

Fig. 1. Statins prevent Pi-induced apoptosis and calcification. HASMC were cultured with the indicated concentrations of fluvastatin and pravastatin in the presence of 2.6 mM Pi for 6 days. Ca deposition was measured by *o*-cresolphthalein complexone method, and normalized by cell protein content. All values are presented as mean± S.E.M. ($n=6$). *$P<0.05$ vs. statin (−) by Fisher's test. N.D. stands for "not detected" (A). On day 6, the inhibitory effect of fluvastatin (0.1 μM) and pravastatin (50 μM) on 2.6 mM Pi [Pi(+)]-induced Ca deposition was evaluated at the light microscopic level with von Kossa's staining (B). Serum-starved HASMC were cultured with the indicated concentrations of fluvastatin and pravastatin for 12 h and then incubated with 2.6 mM Pi for an additional 24 h. A quantitative index of apoptosis, determined by ELISA, is presented as the relative value to that without statins and 2.6 mM Pi. All values are presented as mean±S.E.M. ($n=3$). *$P<0.05$ vs. 2.6 mM Pi, statin (−) by Fisher's test (C). The antiapoptotic effect of fluvastatin (0.1 μM) and pravastatin (50 μM) was evaluated by TUNEL staining (green) on day 6. Nuclei were counterstained with DAPI (4′,6-diamino-2-phenylindole, blue) (D).

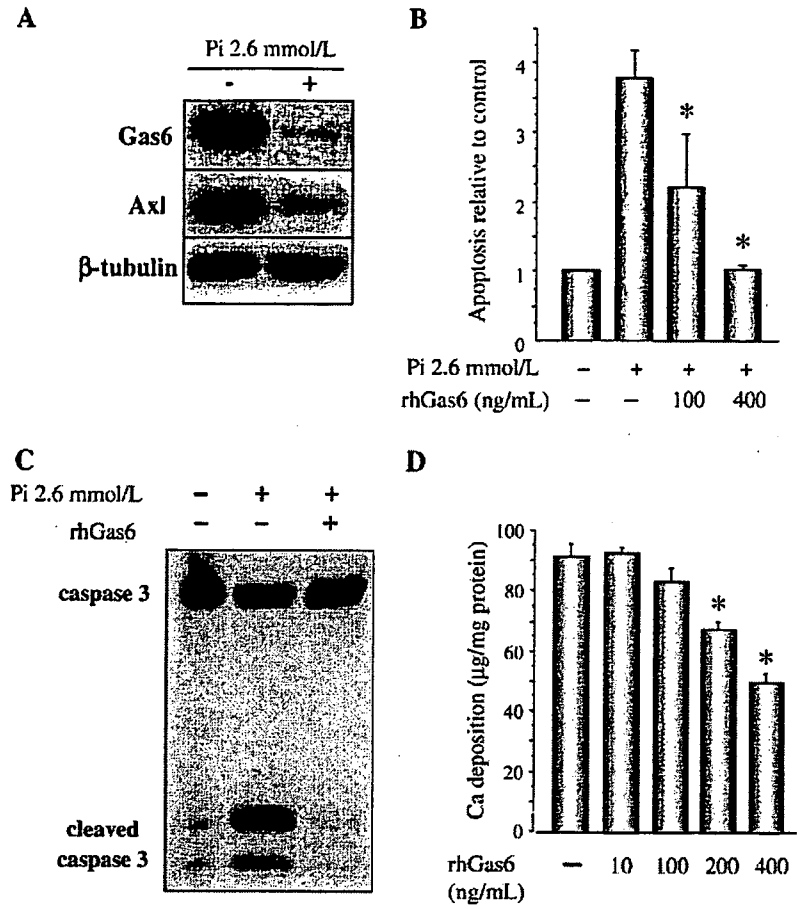

Fig. 2. Pi suppresses Gas6 and Axl expression, and rhGas6 inhibits caspase-dependent apoptosis and calcification. HASMC were cultured in the presence or absence of 2.6 mM Pi for 12 h. Cell lysates were collected and subjected to SDS-PAGE followed by immunoblotting with antibodies to Gas6, Axl or β-tubulin (A). After pretreatment with the indicated concentrations of rhGas6, apoptosis was induced by 2.6 mM Pi. All values are presented as mean±S.E.M. ($n=3$). *$P<0.05$ vs. 2.6 mM Pi, rhGas6 (−) by Fisher's test (B). HASMC were pretreated with rhGas6 (400 ng/ml) for 1 h, then cultured with 2.6 mM Pi for 12 h. Cell lysates were immunoblotted with an antibody that recognizes caspase-3 (35 kDa) and the cleaved forms of caspase-3 (17 and 19 kDa) (C). For measurement of Ca deposition, HASMC were cultured with the indicated concentrations of rhGas6 in the presence of 2.6 mM Pi for 6 days. All values are presented as mean±S.E.M. ($n=6$). *$P<0.05$ by Fisher's test (D). Experiments were performed with at least three different cell populations.

3.3. Downregulation of phospho-Akt participates in Pi-induced apoptosis

Since in NIH-3T3 fibroblasts, the antiapoptotic effect of Gas6-Axl interaction has been shown to be mediated by Akt phosphorylation (Goruppi et al., 1999), we examined whether Akt participates in the signaling of downregulation of the Gas6-Axl interaction during Pi-induced apoptosis. In the presence of 2.6 mM Pi, Akt phosphorylation was downregulated in a time-dependent manner, whereas the expression of total Akt was not changed (Fig. 3A). In addition, rhGas6 abrogated the Pi-induced decrease in Akt phosphorylation, implying that subsequent downregulation of Akt phosphorylation is the pathway of Pi-induced apoptosis (Fig. 3B).

Because Akt phosphorylation is regulated by PI3K, we examined the effect of wortmannin, a specific PI3K inhibitor, on rhGas6-mediated phosphorylation of Akt. As shown in Fig. 3B, wortmannin abrogated the rhGas6-induced phosphorylation of Akt and further eliminated the inhibitory effect of rhGas6 on Pi-induced apoptosis and calcification (Fig. 3C, D). These results indicate that the preventive effect of rhGas6 on Pi-induced apoptosis and calcification was mediated by the PI3K-Akt pathway.

3.4. Pi suppresses Bcl2 phosphorylation and activates Bad

To establish the downstream components of Pi-induced apoptosis, two key apoptosis-regulating proteins, Bcl2 and Bad, were analyzed. During apoptosis, phosphorylation of Bcl2 (active form) and Bad (inactive form) was markedly reduced by 2.6 mM Pi in a time-dependent manner. The expression level of their total protein was not changed in this period (Fig. 4A, B). By supplementation of the medium with rhGas6, the decrease in phosphorylation of Bcl2 and Bad by Pi was reversed to almost the basal level (Fig. 4C, D). These results indicate that Pi promotes apoptosis by inactivating Bcl2 and activating Bad via a Gas6-dependent pathway.

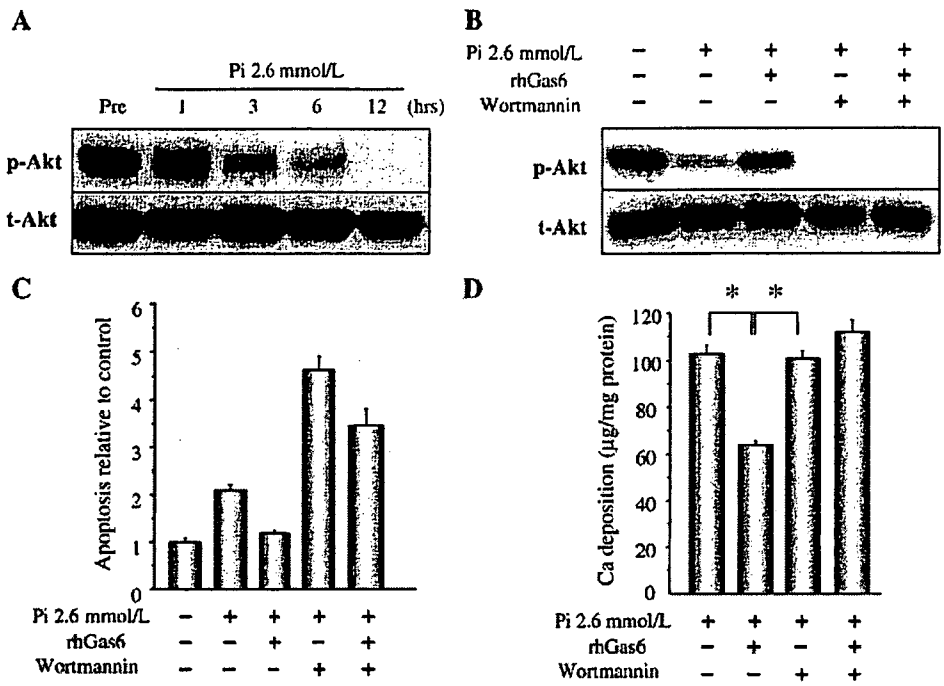

Fig. 3. Pi decreases Akt phosphorylation, and wortmannin abrogates the inhibitory effect of rhGas6 on Akt phosphorylation, apoptosis and calcification. HASMC were cultured in the presence of 2.6 mM Pi for the indicated periods. Cell lysates were immunoblotted with anti-phospho-Akt (p-Akt) antibody and total Akt (t-Akt) antibody (A). HASMC were pretreated with rhGas6 (400 ng/ml), wortmannin (1 μM), or both for 1 h, and then treated with 2.6 mM Pi for 12 h. Cell lysates were immunoblotted with p-Akt and t-Akt antibody (B). After pretreatment with rhGas6 (400 ng/ml) and wortmannin (1 μM), apoptosis was induced by 2.6 mM Pi. All values are presented as mean±S.E.M. ($n=3$). *$P<0.05$ vs. 2.6 mM Pi, rhGas6 (−), wortmannin (−) by Fisher's test (C). HASMC were cultured with rhGas6 (400 ng/ml) and with or without wortmannin (1 μM) in the presence of 2.6 mM Pi for 6 days. Ca content was measured and normalized by cell protein content. All values are presented as mean±S.E.M. ($n=6$). *$P<0.05$ by Fisher's test (D).

3.5. Gas6-mediated survival pathway is the target of statins' effect on apoptosis

To investigate whether the antiapoptotic effect of statins is associated with the Gas6-mediated survival pathway, first, we examined the effect of statins on the expression of Gas6 and Axl. As shown in Fig. 5A and B, both fluvastatin and pravastatin restored the expression of Gas6 and Axl, which was downregulated by 2.6 mM Pi. Because we have shown that the Gas6-mediated survival pathway is Akt-dependent, the effect of statins on Akt phosphorylation was examined. The Pi-induced decrease in Akt phosphorylation was restored by both statins, while total Akt expression was not changed. In addition, we found that both statins stimulated phosphorylation of Bcl2 and

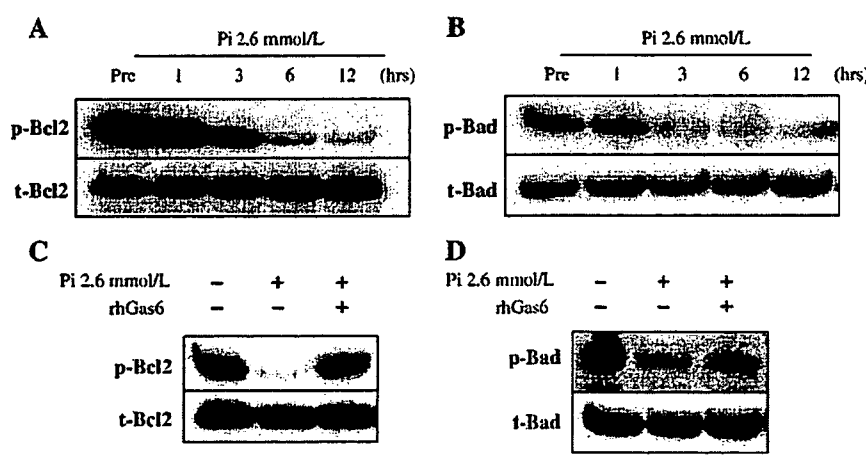

Fig. 4. RhGas6 restores Pi-induced decrease in phosphorylation of Bcl2 and Bad. HASMC were exposed to 2.6 mM Pi for the indicated periods, and cell lysates were subjected to immunoblotting with anti-phospho-Bcl2 (p-Bcl2) antibody and total Bcl2 (t-Bcl2) antibody (A), or with anti-phospho-Bad (p-Bad) antibody and total Bad (t-Bad) antibody (B). HASMC were pretreated with rhGas6 (400 ng/ml) for 1 h, and then treated with 2.6 mM Pi for 12 h. Cell lysates were subjected to immunoblotting with p-Bcl2 and t-Bcl2 antibody (C), or with p-Bad and t-Bad antibody (D).

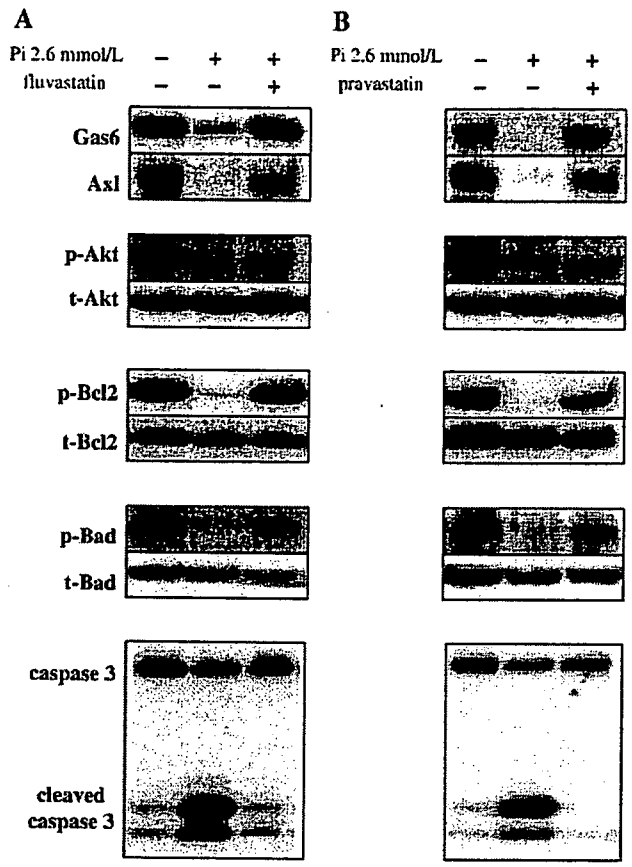

Fig. 5. Antiapoptotic effect of statins is associated with upregulation of Gas6-Axl survival pathway. After pretreatment with 0.1 μM fluvastatin (A) and 50 μM pravastatin (B) for 12 h, apoptosis was induced by 2.6 mM Pi. After 12 h, cell lysates were collected and subjected to SDS-PAGE followed by immunoblotting with antibodies that recognize Gas6 and Axl, with phospho-specific Akt (p-Akt) and total Akt (t-Akt) antibody, with phospho-specific Bcl2 (p-Bcl2) and total Bcl2 (t-Bcl2) antibody, or with phospho-specific Bad (p-Bad) and total Bad (t-Bad) antibody. Cell lysates were immunoblotted with an antibody that recognizes uncleaved caspase-3 (35 kDa) and the cleaved forms of caspase-3 (17 and 19 kDa).

Bad, with total expression unchanged. Pi-induced caspase 3 activation was also prevented by both statins. Taken together, these findings suggest that the inhibitory effect of statins on Pi-induced apoptosis is mediated by restoration of the Gas6-mediated survival pathway; PI3K-induced Akt phosphorylation, Bcl2 activation, Bad inactivation, and caspase 3 inactivation.

4. Discussion

In the present study, we found that both lipophilic fluvastatin and hydrophilic pravastatin protected against Pi-induced apoptosis and calcification in HASMC, as we found with atorvastatin previously. With regard to the different potency of statins, we found that the inhibitory effect of pravastatin was inferior to those of fluvastatin and atorvastatin, which exerted similar effects on calcification and apoptosis. This might relate to our previous finding that the inhibition of calcification by statins was not dependent on the mevalonate pathway (Son et al., 2006). Consequently, the inhibitory effect on calcification was not parallel to the cholesterol-lowering effect. We speculate that the difference between statins was derived from their affinity to *vascular smooth muscle cells* (VSMC), that is, lipophilic statins have stronger effects on VSMC calcification than hydrophilic statins.

The antiapoptotic effect of statins was induced by restoration of the Gas6-mediated survival pathway: PI3K-induced Akt phosphorylation, Bcl2 and Bad phosphorylation, and caspase 3 inactivation. Gas6 plays a crucial role in the effect of statins on Pi-induced apoptosis. Gas6, a secreted vitamin K-dependent protein, binds to the receptors of the mammalian Axl protein-tyrosine kinase family; Axl, Sky, and Mer, with different affinities (Nagata et al., 1996). Gas6 and Axl have been shown to localize in the neointima of the artery after balloon injury, in which they presumably modulate several cell functions such as differentiation, adhesion, migration, proliferation, and survival in a cell-specific manner (Melaragno et al., 1998). The Gas6-Axl interaction is also shown to upregulate scavenger receptor A expression in VSMC (Ming et al., 2001), and facilitates the clearance of apoptotic cells by macrophages (Ishimoto et al., 2000). Of the above functions, protection against apoptotic cell death has been most studied (Goruppi et al., 1996; Healy et al., 2001; Lee et al., 2002; Nakano et al., 1996). Consistently, the expression of Gas6 and Axl was downregulated by Pi, leading to apoptosis and subsequent calcification.

Several intracellular signaling pathways mediated by Gas6-Axl interaction have been shown previously (Goruppi et al., 1999; Lee et al., 2002; Ming et al., 2001). Akt, which is necessary for Gas6-dependent survival, is a critical downstream effector of the PI3K-dependent antiapoptotic pathway. In VSMC, it has been reported that the PI3K-Akt pathway mediates Gas6 induction of scavenger receptor A (Ming et al., 2001). Consistent with these reports, our study provides evidence that the PI3K-Akt pathway is a target of Gas6-Axl interaction, and downregulation of Akt phosphorylation is associated with Pi-induced apoptosis and calcification. Moreover, it is known that PI3K-Akt affects the cell death program through the Bcl2 family of proteins. This protein family is a critical regulator of apoptosis in a variety of cell types, and the balance of antiapoptotic members, such as Bcl2, versus proapoptotic mediators, such as Bad, determines cell fate (Reed, 1997). Bcl2, whose phosphorylation is required for its antiapoptotic activity (Ruvolo et al., 2001), inhibits programmed cell death by several mechanisms: It binds to caspase CED-4 (Apaf-1) and prevents the cell execution cascade; Bcl2 alters mitochondrial membrane potential and inhibits the release of cytochrome c. On the other hand, Bad plays a proapoptotic role in its dephosphorylated form by binding to Bcl2 and reversing its antiapoptotic effect; phosphorylation of Bad results in its cytosolic sequestration by 14-3-3 and hampers its binding to Bcl2 (Zha et al., 1996). It was also reported that Bad is directly phosphorylated by PI3K-Akt (del Peso et al., 1997). In the present study, Bcl2 was inactivated and Bad was activated (both proteins were dephosphorylated) by Pi, directing the cells to apoptosis, and rhGas6 restored phosphorylation of Bcl2 and Bad. During apoptosis, one of the final biochemical events leading to programmed

cell death is activation of the caspase cascade. Activation of caspase 3 is required for internucleosomal DNA degradation (Woo et al., 1998), and caspase inhibition prevents the release of apoptotic bodies from cells (Zhang et al., 1999). In the present study, supplementation of the medium with rhGas6 prevented Pi-induced caspase 3 activation. These results clearly show that Pi downregulates Gas6-Axl, decreases PI3K-mediated Akt phosphorylation, inactivates Bcl2, activates Bad, and activates caspase 3, leading to apoptosis.

The present study demonstrated that statins restored the Gas6-mediated survival pathway. Consistent with these results, Akt phosphorylation has been reported to be an antiapoptotic mechanism of statins: pravastatin inhibited hypoxia-induced apoptosis through activation of Akt in cardiomyocytes (Bergmann et al., 2004), and simvastatin and pravastatin enhanced phosphorylation of Akt and promoted angiogenesis in endothelial cells (Kureishi et al., 2000). Recently, it was reported that statins inhibit caspase 3 activation driven by protein kinase C inhibitors in the process of apoptosis, suggesting that caspase 3 is also under the control of statins during apoptosis (Tanaka et al., 2004).

In this study, we performed experiments under both short-term (within 24 h) and long-term (up to 10 days) conditions. In general, short-term experiments are able to examine acute cell behavior, such as signaling and transcription. However, because obvious HASMC calcification takes at least 3 days, we also performed long-term experiments. Downregulation of Gas6, Axl expression and reduced phosphorylation of Akt, Bcl2, and Bad, and a beneficial effect of statins were consistently found in the long-term condition. This confirms that the Gas6-Axl survival signal is the key mechanism for Pi-induced calcification.

It is concluded that statins inhibit Pi-induced apoptosis via the Gas6/Axl-PI3K-Akt signal pathway, which has a crucial role in the prevention of HASMC calcification. This study adds further evidence of the pleiotropic effects of statins, suggesting a therapeutic strategy for the prevention of vascular calcification.

Acknowledgements

This study was supported by a Grant-in-Aid for Scientific Research from the Ministry of Education, Science, Sports, and Culture of Japan (No. 15390239), Mitsui Sumitomo Insurance Welfare Foundation, Ono Medical Research Foundation, Kanzawa Medical Research Foundation, Novartis Foundation for Gerontological Research, and Takeda Research Foundation. We thank Yuki Ito for technical assistance.

References

Bergmann, M.W., Rechner, C., Freund, C., Baurand, A., Jamali, A., Dietz, R., 2004. Statins inhibit reoxygenation-induced cardiomyocyte apoptosis: role for glycogen synthase kinase 3β and transcription factor β-catenin. J. Mol. Cell. Cardiol. 37, 681–690.

del Peso, L., Gonzalez-Garcia, M., Page, C., Herrera, R., Nunez, G., 1997. Interleukin-3-induced phosphorylation of Bad through protein kinase Akt. Science 278, 687–689.

Eggen, D.A., 1968. Relationship of calcified lesions to clinically significant atherosclerotic lesions. Ann. N. Y. Acad. Sci. 149, 752–767.

Everhart, J.E., Pettitt, D.J., Knowler, W.C., Rose, F.A., Bennett, P.H., 1988. Medial artery calcification and its association with mortality and complications of diabetes. Diabetologia 31, 16–23.

Fridell, Y.W., Villa Jr., J., Attar, E.C., Liu, E.T., 1998. Gas6 induces Axl-mediated chemotaxis of vascular smooth muscle cells. J. Biol. Chem. 273, 7123–7126.

Goodman, W.G., Goldin, J., Kuizon, B.D., Yoon, C., Gales, B., Sider, D., Wang, Y., Chung, J., Emerick, A., Greaser, L., Elashoff, R.M., Salusky, I.B., 2000. Coronary-artery calcification in young adults with end-stage renal disease who are undergoing dialysis. N. Engl. J. Med. 342, 1478–1483.

Goruppi, S., Ruaro, E., Schneider, C., 1996. Gas6, the ligand of Axl tyrosine kinase receptor, has mitogenic and survival activities for serum starved NIH3T3 fibroblasts. Oncogene 12, 471–480.

Goruppi, S., Ruaro, E., Varnum, B., Schneider, C., 1999. Gas6-mediated survival in NIH3T3 cells activates stress signaling cascade and is independent of Ras. Oncogene 18, 4224–4236.

Healy, A.M., Schwartz, J.J., Zhu, X., Herrick, B.E., Varnum, B., Farber, H.W., 2001. Gas6 promotes Axl-mediated survival in pulmonary endothelial cells. Am. J. Physiol., Lung Cell. Mol. Physiol 280, L1273–L1281.

Ishimoto, Y., Ohashi, K., Mizuno, K., Nakano, T., 2000. Promotion of the uptake of PS liposomes and apoptotic cells by a product of growth arrest-specific gene, gas6. J. Biochem. (Tokyo) 127, 411–417.

Kureishi, Y., Luo, Z., Shiojima, I., Bialik, A., Fulton, D., Lefer, D.J., Sessa, W.C., Walsh, K., 2000. The HMG-CoA reductase inhibitor simvastatin activates the protein kinase Akt and promotes angiogenesis in normocholesterolemic animals. Nat. Med. 6, 1004–1010.

Lee, W.P., Wen, Y., Varnum, B., Hung, M.C., 2002. Akt is required for Axl-Gas6 signaling to protect cells from E1A-mediated apoptosis. Oncogene 21, 329–336.

Mark, M.R., Chen, J., Hammonds, R.G., Sadick, M., Godowsk, P.J., 1996. Characterization of Gas6, a member of the superfamily of G domain-containing proteins, as a ligand for Rse and Axl. J. Biol. Chem. 271, 9785–9789.

Melaragno, M.G., Wuthrich, D.A., Poppa, V., Gill, D., Lindner, V., Berk, B.C., Corson, M.A., 1998. Increased expression of Axl tyrosine kinase after vascular injury and regulation by G protein-coupled receptor agonists in rats. Circ. Res. 83, 697–704.

Ming Cao, W., Murao, K., Imachi, H., Sato, M., Nakano, T., Kodama, T., Sasaguri, Y., Wong, N.C., Takahara, J., Ishida, T., 2001. Phosphatidylinositol 3-OH kinase-Akt/protein kinase B pathway mediates Gas6 induction of scavenger receptor a in immortalized human vascular smooth muscle cell line. Arterioscler. Thromb. Vasc. Biol. 21, 1592–1597.

Nagata, K., Ohashi, K., Nakano, T., Arita, H., Zong, C., Hanafusa, H., Mizuno, K., 1996. Identification of the product of growth arrest-specific gene 6 as a common ligand for Axl, Sky, and Mer receptor tyrosine kinases. J. Biol. Chem. 271, 30022–30027.

Nakano, T., Kawamoto, K., Higashino, K., Arita, H., 1996. Prevention of growth-arrest induced cell death of vascular smooth muscle cells by a product of growth arrest-specific gene, gas6. FEBS Lett. 387, 78–80.

Nakano, T., Ishimoto, Y., Kishino, J., Umeda, M., Inoue, K., Nagata, K., Ohashi, K., Mizuno, K., Arita, H., 1997. Cell adhesion to phosphatidylserine mediated by a product of growth arrest-specific gene 6. J. Biol. Chem. 272, 29411–29414.

Neubauer, B., 1971. A quantitative study of peripheral arterial calcification and glucose tolerance in elderly diabetics and non-diabetics. Diabetologia 7, 409–413.

Reed, J.C., 1997. Double identity for proteins of the Bcl-2 family. Nature 387, 773–776.

Ruvolo, P.P., Deng, X., May, W.S., 2001. Phosphorylation of Bcl2 and regulation of apoptosis. Leukemia 515–522.

Son, B.K., Kozaki, K., Iijima, K., Eto, M., Kojima, T., Ota, H., Senda, Y., Maemura, K., Nakano, T., Akishita, M., Ouchi, Y., 2006. Statins protect human aortic smooth muscle cells from inorganic phosphate-induced calcification by restoring Gas6-Axl survival pathway. Circ. Res. 98, 1024–1031.

Tanaka, K., Honda, M., Takabatake, T., 2004. Anti-apoptotic effect of atorvastatin, a 3-hydroxy-3-methylglutaryl coenzyme a reductase inhibitor, on cardiac myocytes through protein kinase C activation. Clin. Exp. Pharmacol. Physiol. 31, 360–364.

Wexler, L., Brundage, B., Crouse, J., Detrano, R., Fuster, V., Maddahi, J., Rumberger, J., Stanford, W., White, R., Taubert, K., 1996. Coronary artery calcification: pathophysiology, epidemiology, imaging methods, and clinical

implications. A statement for health professionals from the American Heart Association. Writing Group. Circulation 94, 1175–1192.

Woo, M., Hakem, R., Soengas, M.S., Duncan, G.S., Shahinian, A., Kagi, D., Hakem, A., McCurrach, M., Khoo, W., Kaufman, S.A., Senaldi, G., Howard, T., Lowe, S.W., Mak, T.W., 1998. Essential contribution of caspase3/CPP32 to apoptosis and its associated nuclear changes. Genes Dev. 12, 806–819.

Yanagita, M., Arai, H., Ishii, K., Nakano, T., Ohashi, K., Mizuno, K., Varnum, B., Fukatsu, A., Doi, T., Kita, T., 2001. Gas6 regulates mesangial cell proliferation through Axl in experimental glomerulonephritis. Am. J. Pathol. 158, 1423–1432.

Zha, J., Harada, H., Yang, E., Jockel, J., Korsmeyer, S.J., 1996. Serine phosphorylation of death agonist BAD in response to survival factor results in binding to 14-3-3 not BCL-X(L). Cell 87, 619–628.

Zhang, J., Reedy, M.C., Hannun, Y.A., Obeid, L.M., 1999. Inhibition of caspases inhibits the release of apoptotic bodies: Bcl2 inhibits the initiation of formation of apoptotic bodies in chemotherapeutic agent-induced apoptosis. J. Cell Biol. 145, 99–108.

泌尿器外科　2007年
20(臨増), 473～475

1. テストステロンとメタボリックシンドローム

秋下　雅弘

東京大学大学院医学系研究科加齢医学*

はじめに

メタボリックシンドローム（MetS）は，内臓肥満あるいはインスリン抵抗性を基盤として，高血圧，脂質代謝異常（高トリグリセリド血症あるいは低HDLコレステロール血症），耐糖能異常が合併した病態である。たとえ各因子が軽症であっても，それらの重複により心筋梗塞など動脈硬化性疾患の発症リスクが著しく高くなることが問題で，働き盛りの中高年男性に罹患率が高い。この年代は，Late-onset hypogonadism（LOH）の好発する集団でもあり，テストステロン(T)とMetSとの関係には興味が持たれる。

従来，エストロゲンの抗動脈硬化作用に対してTは動脈硬化促進的に働くと考えられてきた。しかし最近では，高齢男性におけるT濃度の低下が動脈硬化性疾患や代謝異常の危険因子であることが指摘されるようになった。本稿では，日本人男性でもT低下がMetSと関連することを示し，その意味について考察する。

I. テストステロン濃度とMetSとの関連

30～69歳の男性患者118名を対象に，血清T濃度とMetSの診断およびその構成要素との関連を調べた。糖尿病患者は除外したが，高血圧や高脂血症など他の生活習慣病患者は含む。日本のMetS診断基準に従い，臍周囲径85cm以上で，血圧高値（収縮期≥130mmHgまたは拡張期≥85mmHg），脂質代謝異常（トリグリセリド≥150mg/dlまたはHDLコレステロール≤40mg/dl），空腹時高血糖（≤110mg/dl）のうち2つ以上を有する場合をMetSと診断し，また腹囲を含む各因子の保有数をカウントした。

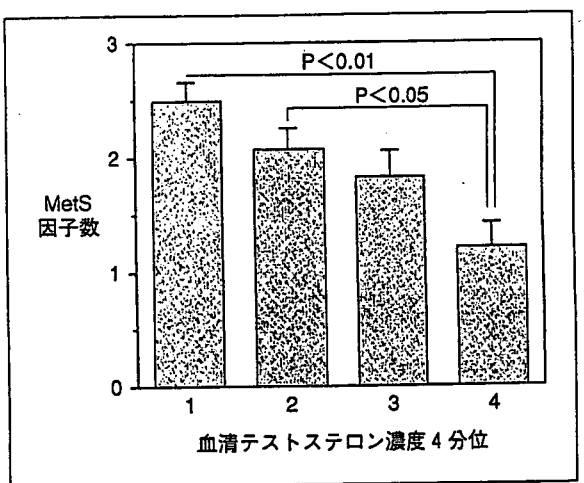

図1　中高年男性における総テストステロン濃度とメタボリックシンドローム因子数（腹部肥満，血圧高値，脂質異常，血糖高値）との関連

図1に示すように，総T濃度で4分位すると，低値ほどMetS因子の保有数が多く，逆にMetS因子数が多いほど総テストステロン濃度は低かった。また，年齢調整したロジスティック回帰分析では，総T濃度4分位の1階層低下により，MetS診断に対する相対リスクは1.61倍（95%信頼区間1.11～2.34）に増加した。

Testosterone and metabolic syndrome
Masahiro Akishita
Department of Geriatric Medicine, Graduate School of Medicine, The University of Tokyo

key words：アンドロゲン，肥満，性腺機能低下症

* 文京区本郷7-3-1（03-5800-8652）〒113-8655

表1 メタボリックシンドローム指標に対する総テストステロン濃度の寄与度

	従属変数	標準回帰係数	p値
肥満	Body mass index	−0.366	<0.001
	ウエスト周囲径	−0.378	<0.001
	ウエスト／ヒップ比	−0.383	<0.001
血圧	収縮期血圧	−0.315	<0.001
	拡張期血圧	−0.226	0.012
脂質	遊離脂肪酸	−0.237	0.018
	トリグリセリド	−0.207	0.026
	HDLコレステロール	0.065	0.490
	LDLコレステロール	0.001	0.992
糖代謝	空腹時血糖	−0.231	0.011
	ヘモグロビンA1c	−0.211	0.020
	HOMA-IR	−0.305	0.002

総テストステロン濃度と年齢を独立変数とし，表のいずれかを従属変数とした重回帰分析

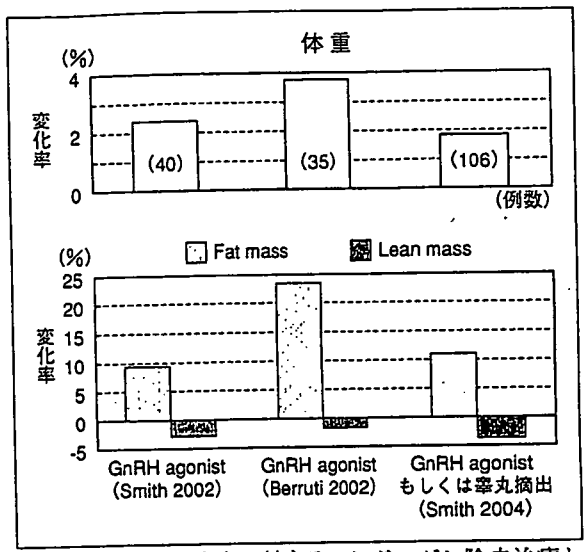

図2 前立腺ガン患者に対するアンドロゲン除去治療と1年後の体格変化：3研究のまとめ（文献3より引用）

次に，MetSの各因子に関係する測定値がT濃度と関連するかどうかを検討した（表1）。年齢調整した重回帰分析で検討したところ，総T濃度はHDLコレステロールを除くすべての項目に対して有意な説明変数であった（LDLコレステロールは本来MetSとは独立した動脈硬化危険因子である）。つまり，総T濃度の低い中高年男性は，腹部肥満があり，血圧が高く，トリグリセリドが高く，空腹時血糖が高いという結果である。また，インスリン抵抗性指標HOMA-IRや遊離脂肪酸濃度ともテストステロン濃度が関連しており，MetS成立過程の上流にTが関与する可能性を示唆する。

II T低下はMetSの原因か結果か？

さて，それでは本当にT低下がMetSの原因となるのか，あるいは肥満やMetSの結果として性腺機能が低下するのかという疑問がある。臨床的には縦断観察研究と介入研究だけがこの問いに答えられるが，実は双方の因果関係について，それも同一のグループが報告している[1,2]。フィンランドで行われた中年男性（平均51歳）の疫学研究では，11年間の追跡期間中に21％がMetSを，8％が糖尿病を発症したが，開始時のT濃度が下位1/4の群では，年齢調整後の発症率がMetS，糖尿病ともに2.3倍であった[1]。逆に，開始時にMetSの診断基準を満たした者は11年間にT低下症のリスクが2.6倍であった[2]。

前立腺ガンに対してT除去療法が行われるが，その際のT低下と関連して肥満がみられることも報告されている。Smithによる3研究のまとめ[3]を図2に示すが，対照群がないため厳密な比較は困難なものの，T除去療法開始後1年で数％の体重増加と十数％の体脂肪増加を認めている。逆に，MetS患者あるいは肥満者にT補充療法を行うと改善するかどうかであるが，MetSの各指標をきちんと検討した研究はない。ただ，高齢男性に対するT補充療法により体脂肪の減少がみられることは，小規模ではあるがプラセボ対照研究[4]でも示されている。最後に，肥満者が痩せるとTが増加するかどうかであるが，運動療法によりTが増加することは数多く報告されている。また，中年男性を食事療法により9週間で十数キログラム痩せさせたところ，遊離T濃度が増加したとの報告がある[5]。

まとめ

日本人中高年男性でも，T低下とMetSが合併することは確かなようである。ただ，因果関係については両方向の可能性があるため，MetS患者に対してむやみにT補充療法を行えばよいとは言えない。むしろ現時点で確実な方法は食事・運動療法により減量することである。ただ，LOHのため肥満者にT補充療法を行う場合には，体脂肪の減少やそれに伴う糖・脂質代謝改善も期待してよいのではなかろうか。

文　献

1) Laaksonen DE, Niskanen L, Punnonen K, et al: Testosterone and sex hormone-binding globulin predict the metabolic syndrome and diabetes in middle-aged men. Diabetes Care **27**: 1036-1041, 2004
2) Laaksonen DE, Niskanen L, Punnonen K, et al: The metabolic syndrome and smoking in relation to hypogonadism in middle-aged men: a prospective cohort study. J Clin Endocrinol Metab **90**: 712-719, 2005
3) Smith MR: Osteoporosis and obesity in men receiving hormone therapy for prostate cancer. J Urol **172**: S52-6, 2004
4) Snyder PJ, Peachey H, Hannoush P, et al: Effect of testosterone treatment on body composition and muscle strength in men over 65 years of age. J Clin Endocrinol Metab **84**: 2647-2653, 1999
5) Niskanen L, Laaksonen DE, Punnonen K, et al: Changes in sex hormone-binding globulin and testosterone during weight loss and weight maintenance in abdominally obese men with the metabolic syndrome. Diabetes Obes Metab **6**: 208-215, 2004

性ホルモン補充療法(HRT)

秋下雅弘

Risks and benefits of hormone replacement therapy

Masahiro Akishita
Department of Geriatric Medicine, Graduate School of Medicine, University of Tokyo

Abstract

In contrast to observational studies, clinical trials examining the efficacy of hormone replacement therapy (HRT) have shown the overall negative or deteriorating effects of HRT in postmenopausal women. Particularly, the results of Women's Health Initiative (WHI) demonstrated that HRT was preventive of fractures and colon cancer but increased the risk of myocardial infarction, stroke and dementia in addition to breast cancer and venous thromboembolism. Conversely, recent progress in androgen research suggests the efficacy of androgen replacement therapy in elderly men, pending clinical trials.

Key words: estrogen, androgen, menopause, atherosclerosis, osteoporosis

はじめに

内因性の女性ホルモン，特にエストロゲンは女性の老化を抑え健康を保つ働きを有するようである．この点は，更年期障害だけでなく動脈硬化性疾患や骨粗鬆症などの老年疾患が閉経と関連して増加すること，人工的閉経がヒトや動物に病的状態を惹起することからも明らかである．このような閉経に伴う異常を是正する目的でエストロゲン補充療法が実施されるが，実際にはエストロゲンによる子宮癌の増加を抑える目的でプロゲスチン製剤を併用することが多いので，ホルモン補充療法(hormone replacement therapy：HRT)と呼ばれる．我が国では2％程度の閉経後女性が実施しているにすぎないが，北米では20％以上，欧州や韓国，台湾でも10％以上もの女性が行っている．

HRTの長期効果について，HRTを行っている女性と行っていない女性とを比較した観察研究の結果は数多く報告されているが，心筋梗塞や脳卒中などの動脈硬化性疾患，骨粗鬆症，認知症など総じてHRTの有効性を支持するものであった．しかし，乳癌による死亡までが少ないことに示されるように(表1)[1]，HRTを通じた医療管理自体の効果など薬効以外のバイアスも考えられる．実際，HRT施行者の方が非施行者に比べて教育レベルが高く裕福であり，元来健康であるという点が交絡因子として指摘され，純粋に薬効を評価するために大規模無作為比較試験が実施された．その結果はHRTの多面的効果を否定するものであり，特に2002年に最初の報告がなされたWomen's Health Initiative (WHI)[2]はインパクトも強く，HRTの有効性と安全性について議論が沸き起こった．

東京大学大学院医学系研究科 加齢医学

0047-1852/08/¥40/頁/JCLS

表1　総死亡および主要疾患による死亡に及ぼすHRTの影響(観察研究の結果)

死亡原因	女性ホルモン使用歴		
	非使用者	現使用者	使用歴有
全死亡原因	1.0	0.63	1.03
冠動脈疾患	1.0	0.47	0.99
脳卒中	1.0	0.68	1.07
がん全体	1.0	0.71	1.04
乳癌	1.0	0.76	0.83

Nurses' Health Study(1976-1994)
(文献[1]より改変)

本稿では，HRTのリスクと利点を解説し，現時点でのHRTの適応について述べる．また，最近注目されている男性のアンドロゲン補充療法(androgen replacement therapy: ART)についても簡単に触れる．

1. HRTの大規模比較試験とその解釈

HRTの長期効果をみたプラセボ対照大規模比較試験はHeart and Estrogen/Progestin Replacement Study(HERS)[3]とWHIの2つである．その他の試験は，WHIの結果を受けて解析前に中止されたか短期効果の評価にとどまる．HERSは冠動脈疾患患者を対象とした試験で，プロゲスチン併用HRTで平均4.1年間フォローし，冠動脈疾患再発も脳卒中発症もプラセボと同等であった．骨折，がんの発生も両群で変わらなかったが，HRTにより静脈血栓症は2.89倍，胆のう疾患は1.38倍に増加した．WHIでは，基本的に冠動脈疾患をもたない閉経後女性を対象にHERSと同じ併用HRTの有用性を検討した．平均5.2年間の追跡期間中，HRTにより乳癌，静脈血栓症・肺塞栓症のみならず，冠動脈疾患は1.29倍に，脳卒中も1.41倍に増加してしまった(図1)．それまで証明されていなかった(恐らく骨粗鬆症に対する効果を介した)骨折と大腸癌の減少を認めたものの，総合評価として閉経後女性にHRTは好ましくない治療であるとされた．その後，子宮を摘出した女性を対象とした結合型エストロゲン単独療法によるWHIのサブ解析結果[4]が報告され，乳癌，冠動脈疾患，大腸癌はプラセボと同等になり，やはり肺塞栓症は1.34倍，脳卒中は1.39倍に増加，骨折は0.61倍に減少という結果であった．プロゲスチン併用に比べてエストロゲン単独の方が全体的に良好な結果ではあるが，動脈硬化性疾患への効果を含めプラセボに勝ることはできなかった．更に，やはり観察研究では予防的効果が指摘されていた認知症に対する効果も，WHI Memory Study[5]では否定され，むしろ併用HRTおよびエストロゲン単独療法により悪化する傾向であった．

WHIの結果については我が国のマスコミにも報道され，特に乳癌の問題が取り沙汰された．しかし，HRTによる乳癌と静脈血栓症・肺塞栓症の発生増加は予想された範囲内であり驚くべきことではない．全く予想外であったのは，冠動脈疾患や脳卒中，認知症に効果がないばかりかむしろ悪いという結果であり，その点が議論の的となった．まず，静脈血栓症の原因となるエストロゲンの凝固・線溶系活性化が動脈系でも血栓形成に作用する可能性がある．次に，CRP増加にみられる催炎症作用がプラークの不安定化・破綻をもたらす可能性がある．更に，以前は無害とされていたエストロゲンによるトリグリセリド増加作用も，small, dense LDLの増加と関連して動脈硬化促進的に作用すると考えられるようになった．つまり，心血管系に対してもエストロゲンは好ましい作用ばかりでなく好ましくない作用を有し(表2)，状況によって悪い作用が前面に出てしまうと考えられる．血管性認知症ばかりでなくAlzheimer型認知症にも脳血管循環が関係することがわかっており，認知症に対する効果も血管系への悪影響が及んだ可能性が高い．

一方，2つの試験で検討されたHRTが，最も標準的な処方である結合型エストロゲン0.625 mg/日と酢酸メドロキシプロゲステロン2.5mg/日の連日併用のみであることに対する疑問がある．子宮癌の予防目的で併用されるプロゲスチンは内皮機能などエストロゲンの効果を打ち消すことが報告されており，乳癌にも悪影響があるとされる(WHIにおける併用と単独HRTの差)．また，上述した凝固・線溶系，炎症，トリ

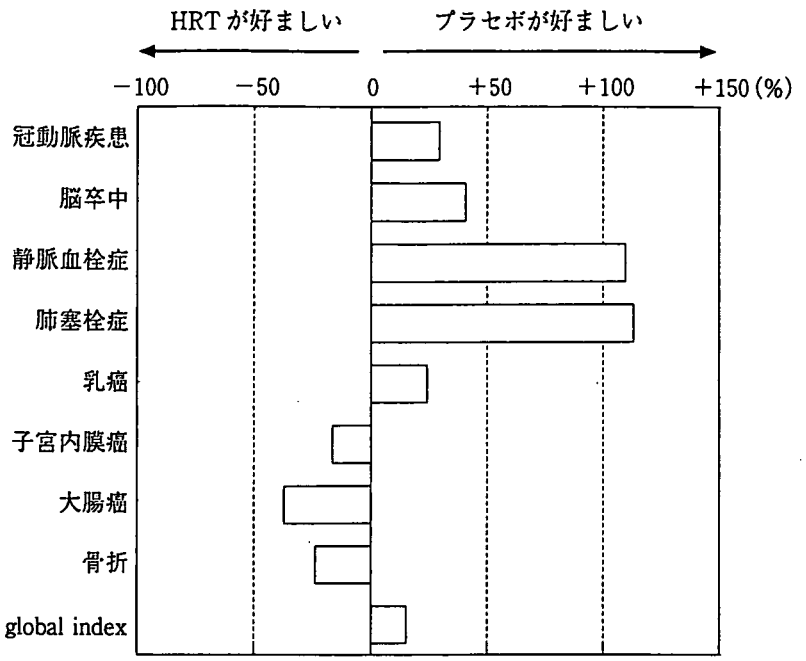

図1 Women's Health Initiativeにおけるエンドポイントと HRTの効果
(文献[2]より引用)

表2 心血管疾患に関係するエストロゲンの作用

	好ましいもの	好ましくないもの
脂質	LDL-C減少 HDL-C増加	トリグリセリド増加 small, dense LDL増加
凝固・線溶系	PAI-1低下 フィブリノゲン低下	プロトロンビンフラグメント増加 VII因子増加 アンチトロンビンIII低下
炎症/接着	接着分子低下	CRP増加
血圧/心血管	ACE活性低下 内皮依存性血管拡張作用 NO増加 ET-1低下, PGI_2増加 平滑筋細胞遊走・増殖抑制	アンジオテンシノーゲン増加

グリセリドに対する悪影響はほとんど肝臓を介する作用であり，肝臓の初回通過効果がない貼付型エストラジオールでは，これらの有害作用は少ない．用量も多いという意見があり，実際に半量HRTで検討すると，凝固・線溶系，血清トリグリセリドおよびLDL小粒子化への影響は少なく，血管内皮機能改善作用や脳血流増加は同等に認められた．

対象についても，HERSでは平均67歳，WHIでも平均63歳という高齢女性であったことに対して，その結果を更年期の女性まで拡大して適応することへの批判がある．実際，最近のWHIサブ解析[6]では，閉経後まもなくHRTを開始した場合には，心血管疾患，特に冠動脈疾患の発症は抑制される可能性が示された．更に，HERSはもちろんWHIの症例も動脈硬化のハイリスク群であり，WHIの症例はbody mass index ≧25という我が国では肥満に分類される症例が約2/3，HRT施行歴のある症例が約1/4，喫煙歴のある症例が約半数と，我が国の閉経後